

Materials informatics based on evolutionary algorithms: Application to search for superconducting hydrogen compounds

Takahiro Ishikawa,^{1,2,*} Takashi Miyake,³ and Katsuya Shimizu²

¹*ESICMM, National Institute for Materials Science, 1-2-1 Sengen, Tsukuba, Ibaraki 305-0047, Japan*

²*Center for Science and Technology under Extreme Conditions,
Graduate School of Engineering Science, Osaka University,
1-3 Machikaneyama, Toyonaka, Osaka 560-8531, Japan*

³*CD-FMat, National Institute of Advanced Industrial Science and Technology,
1-1-1 Umezono, Tsukuba, Ibaraki 305-8568, Japan*

(Dated: August 5, 2019)

We present materials informatics approach to search for superconducting hydrogen compounds, which is based on a genetic algorithm and a genetic programming. This method consists of four stages: (i) search for stable crystal structures of materials by a genetic algorithm, (ii) collection of physical and chemical property data by first-principles calculations, (iii) development of superconductivity predictor based on the database by a genetic programming, and (iv) discovery of potential candidates by regression analysis. By repeatedly performing the process as (i) \rightarrow (ii) \rightarrow (iii) \rightarrow (iv) \rightarrow (i) \rightarrow ..., the superconductivity of the discovered candidates is validated by first-principles calculations, and the database and predictor are further improved, which leads to an efficient search for superconducting materials. We applied this method to hypothetical ternary hydrogen compounds and predicted KScH_{12} with a modulated hydrogen cage showing the superconducting critical temperature of 122 K at 300 GPa and GaAsH_6 showing 98 K at 180 GPa.

PACS numbers: 61.50.Ah, 74.10.+v, 74.62.Fj, 74.70.jb, 74.70.Dd

I. INTRODUCTION

The use of an informatics approach to materials science, *i.e.* materials informatics (MI), has been expected to bring the acceleration for the exploration of new materials¹⁻⁴. High-throughput screening and machine learning have been employed to discover hidden trends and create predictive models in databases of physical and chemical properties for crystalline compounds, *e.g.* search for cathode materials with a long cycle life for lithium-ion battery⁵ and new superconducting materials⁶.

Search for new physical and chemical properties have been performed by varying compositions and external parameters such as pressure, temperature, and electromagnetic field with respect to already known materials. These approaches are considered as the exploration of optimal solutions in vast and complicated search space under given conditions. In such a case, evolutionary algorithm (EA), which is a heuristic-based approach to solving problems using mechanisms inspired by biological evolution, *e.g.* mating, mutation, selection, inheritance, *etc.*, is effective for the discovery of the optimal solutions. EA has been used in a wide variety of scientific research fields and has been applied to search for stable or metastable crystal structures⁷⁻¹¹, well-performed mathematical equations and computer programs in predefined task, and so on.

In this study, we propose materials informatics approach to search for new functional materials, which is based on a genetic algorithm (GA) and a genetic programming (GP) included in the EA techniques (Fig. 1). This method consists of four stages: (i) determination

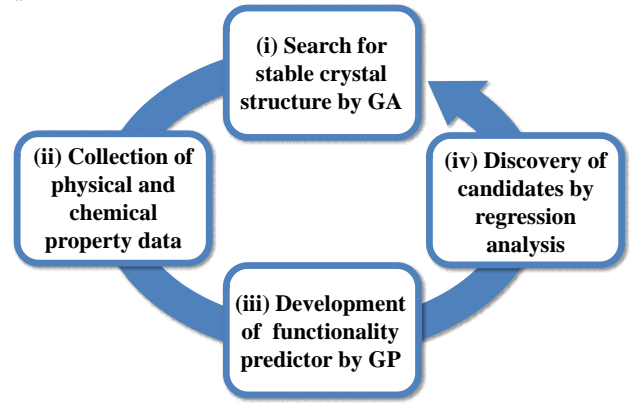


FIG. 1: (Color online) Materials informatics approach to search for new functional materials, which is based on the genetic algorithm (GA) and the genetic programming (GP).

of stable crystal structures of materials by GA, (ii) collection of physical and chemical property data by performing first-principles calculations and development of database, (iii) development of a functionality predictor based on the data by GP, and (iv) discovery of potential candidates by regression analysis. By repeatedly performing the process as (i) \rightarrow (ii) \rightarrow (iii) \rightarrow (iv) \rightarrow (i) \rightarrow ..., the candidates discovered at the stage (iv) are validated by first-principles calculations through (i) to (ii), and the database and predictor are gradually improved using the validation results. Thus, this method enables to accelerate the search for new functional materials. This paper is organized as follows: the details of GA for crystal structure search and GP for predictor de-

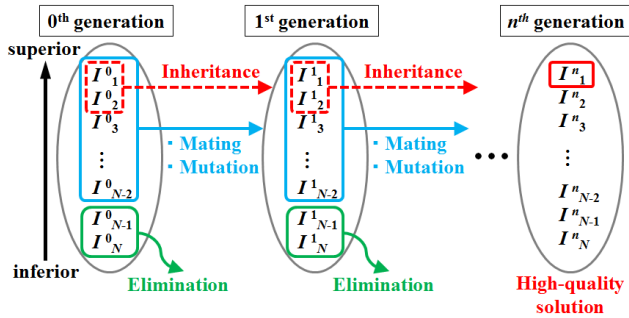


FIG. 2: (Color online) Schematic view of evolutionary algorithm. I represents an individual, and N is the number of individuals in the population.

velopment are presented in Sec. II, the application of our MI method to the search for superconducting hydrogen compounds is shown in Sec. III, and the discussion and conclusion are drawn in Sec. IV.

II. EVOLUTIONARY ALGORITHMS

Figure 2 shows a process on the search for high-quality optimal solutions by EA. First, we prepare for a population consisting of individuals (I), which are generated randomly and ranked according to a fitness parameter (0th generation). Then, few especially inferior individuals are eliminated from the population (elimination), and the other ones are used for the creation of new individuals for the next generation. The new individuals are created by randomly applying evolutionary operations, “mating” and “mutation”. Few especially superior individuals are inherited to the next generation (inheritance), and all the individuals are ranked again. By repeatedly performing this process, the population is evolved to more superior one and finally high-quality optimal solutions are obtained. As mentioned above, in our MI approach, we use GA to search for stable crystal structures at the stage (i), and GP to develop a functionality predictor at the stage (iii).

A. GA for crystal structure search

Figure 3 shows a flowchart at each generation with respect to the structure search by GA. For the evolutionary operators, the mating is the operator to create a slab structure from randomly selected two individuals (Fig. 4 (a)) and the mutation is the operator to give a lattice distortion or an atomic permutation for randomly selected an individual (Fig. 4 (b))¹¹. All the structures generated randomly or created by the mating and mutation are optimized at a given pressure, and the enthalpies, *i.e.* $H = E + PV$, are calculated using total energy E , pressure P , and volume V . Then, the population for the next generation is constructed by inheriting the few

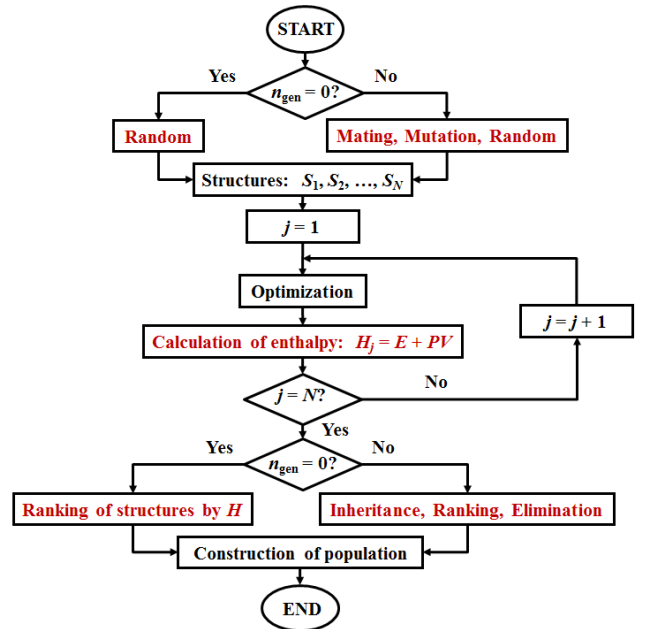


FIG. 3: (Color online) Flowchart at each generation with respect to crystal structure prediction by GA.

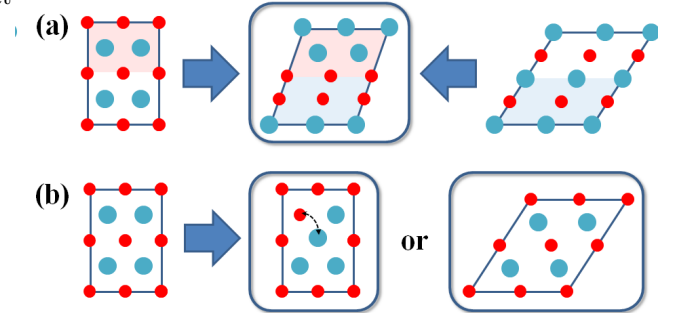


FIG. 4: (Color online) Schematic view of crystal structure search by the evolutionary operations: (a) mating and (b) mutation.

elite structures with especially lower enthalpy at the previous generation, ranking all the structures according to the enthalpy, and eliminating few inferior structures with especially higher enthalpy from the population. Once the stable structures are obtained, physical and chemical property data are collected using first-principles calculations (the stage (ii) in Fig. 1). The calculated results are aggregated in the database.

B. GP for predictor development

Figure 5 shows a flowchart at each generation with respect to the development of the predictor by GP. GP is an expansion of GA where individuals are represented as computer programs or mathematical functions using tree structures as shown in Fig. 6. The tree structure consists

of branch and leaf nodes, and in our GP search, a branch node depicts an element from arithmetic operators (+, −, ×, ÷) and a leaf node depicts an element from constants (1-10) and variables to develop mathematical functions. For example, the left tree of Fig. 6 (a) represents the function of $f(A, B) = \{(3 + A) \div 4\} \times \{(1 - 2) + B\}$, which is written as $f(A, B) = \times \div + 3 A 4 + - 1 2 B$ in the Polish notation to deal with arithmetic expression in programming language. The mating is the operator to create new tree structures by exchanging branches between two individuals selected randomly (Fig. 6 (a)) and the mutation is the operator to exchange branches within an individual (Fig. 6 (b)). The individuals are ranked according to the strength of the correlation between the value obtained by substituting the datasets into the function (evaluation value: x) and physical property data which we will investigate (y). The correlation coefficient (r) between x and y is calculated by $r = s_{xy} / s_x s_y$, using the data included in the database. The parameters s_x , s_y , and s_{xy} are a standard deviation of data x , that of y , and a covariance between x and y , respectively. They are calculated as follows:

$$s_x = \left(\frac{1}{m} \sum_{i=1}^m (x_i - \bar{x})^2 \right)^{1/2}, \quad (1)$$

$$s_y = \left(\frac{1}{m} \sum_{i=1}^m (y_i - \bar{y})^2 \right)^{1/2}, \quad (2)$$

and

$$s_{xy} = \frac{1}{m} \sum_{i=1}^m (x_i - \bar{x})(y_i - \bar{y}), \quad (3)$$

where m is the number of the datasets used for the calculation, and \bar{x} (\bar{y}) is the average value of x (y). Then, similarly to the case of the structure search, a high-quality function is developed by repeatedly performing the evolution, *i.e.* inheriting, ranking according to the absolute value of r ($|r|$), and eliminating.

For a number of high-quality functions obtained by several GP searches, the predictive ability of the function is checked by a k -fold cross-validation¹². The datasets are randomly divided into k subsets, and a single subset is retained as the validation data for testing the functions and the remaining $k - 1$ subsets are used for training the functions. In this study, we used $R = |r_{ts}|$ for the evaluation of the predictive ability, where r_{ts} represents the correlation coefficient calculated from the testing data and takes the value from 0 to 1. If the function developed by GP gives the strong correlation not only for the training data but also the testing data, then R shows a large value. This process is repeated k times by rotation and the values of R are averaged (\bar{R}). The function with the largest \bar{R} is adopted as the predictor of the physical property which we will investigate. At the stage (iv), potential candidates are selected by the regression analysis using the predictor.

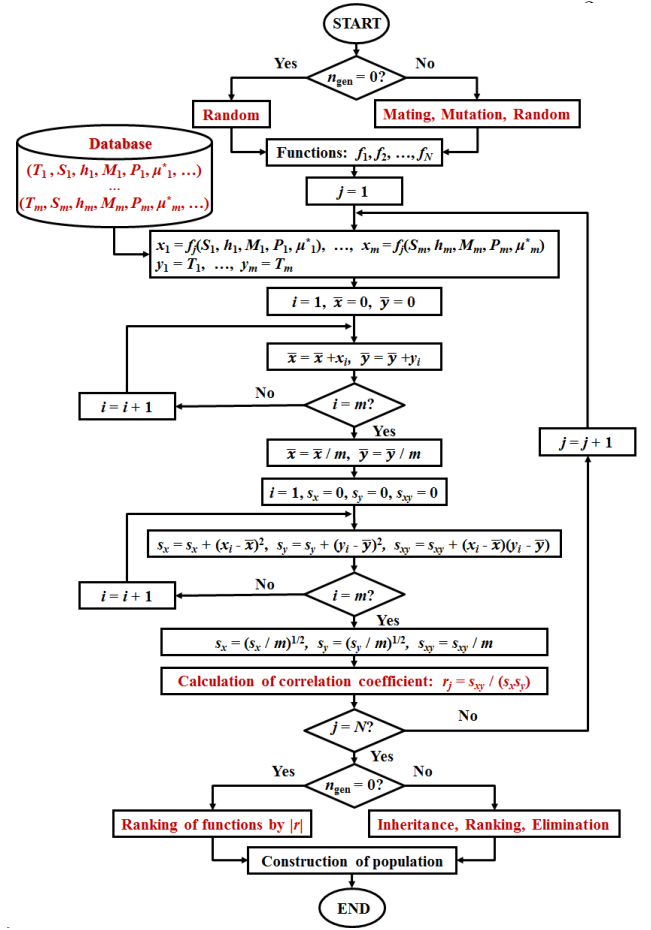


FIG. 5: (Color online) Flowchart at each generation with respect to functionality predictor development by GP. The case of the superconductivity is shown as an example of the functionality (see Sec. III B).

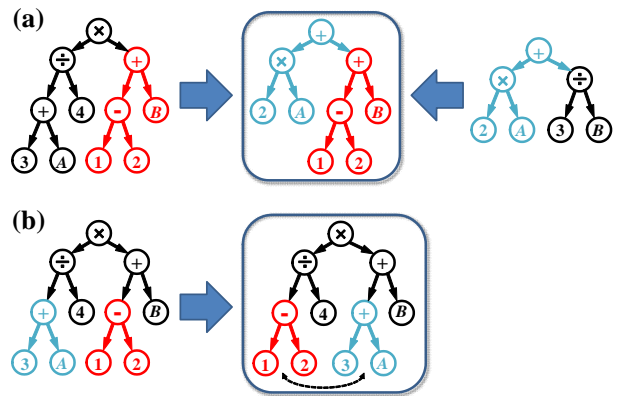


FIG. 6: (Color online) Schematic view of mathematical function development by evolutionary operations: (a) mating and (b) mutation.

III. APPLICATION TO SEARCH FOR SUPERCONDUCTING HYDROGEN COMPOUNDS

We developed the calculation codes for the above GA and GP searches and applied our MI method to search for superconducting hydrogen compounds. In 2015, high-temperature superconductivity was discovered in hydrogen sulfide (H_2S) under high pressure and the superconducting critical temperature T_c reaches 203 K at pressure of 155 GPa¹³. In 2018-2019, compressed lanthanum hydrides broke the record and the superconductivity was observed at 250 K at 170 GPa by Drozdov *et al.*¹⁴ and 260 K at 190 GPa by Somayazulu *et al.*¹⁵. Therefore, other hydrogen compounds also have a potential to become similar high- T_c superconductors under some conditions. However, there are a huge number of combinations for hydrogen compounds in multicomponent system. For example, there exist 13572 combinations for ternary hydrogen compounds formed by all elements with the atomic numbers from 2 to 118, and the number is much further increased by taking stoichiometry and crystal structure into account. Therefore, the MI approach is of great help to discover potential candidates with the high- T_c superconductivity.

A. Collection of superconductivity data: stage (ii) in MI cycle

First we developed the database by collecting the first-principles calculation data with respect to chemical composition, crystal structure, and superconducting property of binary hydrogen compounds under high pressure condition from literature^{16–78}. The database includes 497 datasets for the compounds with 62 elements colored in the periodic table of Fig. 7. We used only the T_c data obtained by the Allen-Dynes formula⁷⁹ in this study, which are all plotted in the lower panel of Fig. 7. The highest T_c value for each binary system is represented as a histogram. The superconductivity of $T_c \geq 200$ K is predicted in the following compounds: $T_c = 265$ K at 250 GPa in YH_{10} ⁶⁷, 263 K at 300 GPa in MgH_6 ⁴⁸, 238 K at 210 GPa in LaH_{10} ⁶⁷, 206 K at 150 GPa in CaH_{12} ⁷⁴, 204 K at 200 GPa in AcH_{10} ⁷⁵, and 204 K at 200 GPa in H_3S ³². Figure 8 shows the relationships between T_c and hydrogen concentration, mass per atom, pressure, and space group number for all the data included in the database. Although large hydrogen concentration, light mass, and high pressure favor the increase of the superconductivity, they are not a necessary and sufficient condition for high- T_c superconductivity. Further, space group number, *i.e.* crystal symmetry, shows a weak correlation with T_c . The data suggests that the search for hydrogen compounds with high T_c is seemingly simple, but it is actually difficult just to investigate these parameters independently.

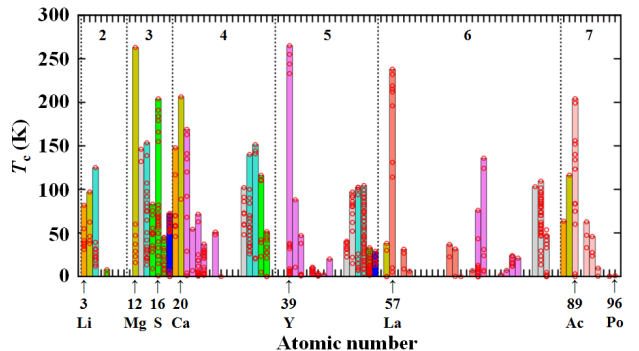
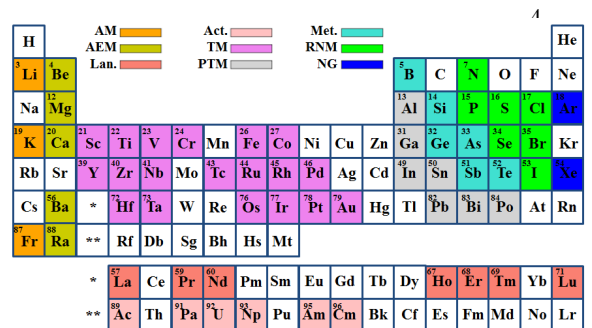


FIG. 7: (Color online) Elements forming the binary hydrogen compounds included in the database and all the T_c data. The elements are divided into nine groups using different colors: alkali metal (AM), alkaline earth metal (AEM), lanthanide (Lan.), actinide (Act.), transition metal (TM), post-transition metal (PTM), metalloid (Met.), reactive nonmetal (RNM), and noble gas (NG).

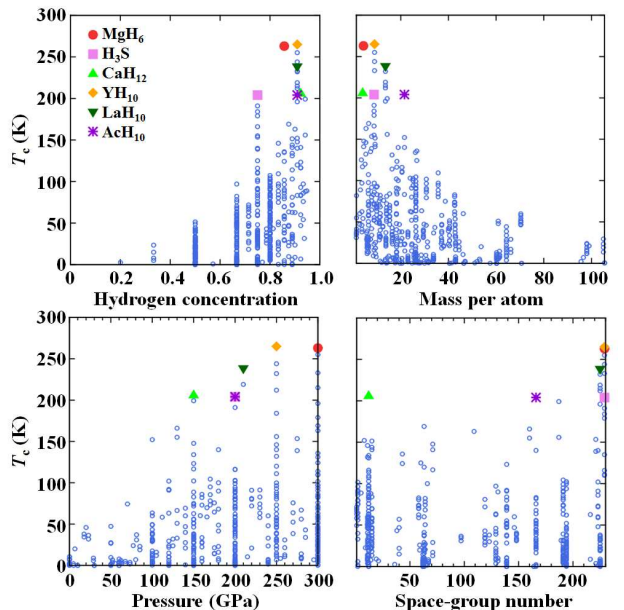


FIG. 8: (Color online) Relationships between the superconducting T_c and hydrogen concentration (top left), T_c and mass per atom (top right), T_c and pressure (bottom left), and T_c and space-group number (bottom right) for superconducting binary hydrogen compounds predicted by first-principles calculations.

B. Development of superconductivity predictor: stage (iii) in MI cycle

Next we developed the superconductivity predictor by GP using the datasets included in the database. The datasets were divided into ten subsets for the cross-validation, *i.e.* $k = 10$, and 90% of the data for training and 10% for testing. We used five variables, space group (S), hydrogen concentration (h), mass per atom (M), pressure (P), and the effective screened Coulomb repulsion constant in the Allen-Dynes formula⁷⁹ (μ^*), to obtain the superconductivity evaluation value x ; $x = f(S, h, M, P, \mu^*)$ (see Fig. 3). The functions are evolved for 5000 generations, based on the correlation to the superconducting T_c (T); $y = T$. The number of the individuals were set at 20, in which 8 functions are created by the mating, 8 by the mutation, 2 are randomly generated, and 2 are inherited. Then the 10-fold cross-validation was carried out and the \bar{R} value was calculated. We performed this process 50 times in parallel and adopted the function with the largest \bar{R} as the superconductivity predictor. Figure 9 shows the correlation between T_c and x obtained by the predictor. $|r_{tr}|$ and $|r_{ts}|$ are 0.78 and 0.81, respectively, where r_{tr} represents the correlation coefficient calculated from the training data and takes the value from 0 to 1. The compounds taking small x values are potential candidates for the high- T_c superconductivity. See Ref. 80 with respect to the details of the predictor, in which the function is represented as the Polish notation.

C. Search for potential candidates: stage (iv) in MI cycle

We searched for the potential candidates in ternary hydrogen compounds using this predictor. First, we created 497 datasets for ternary hydrogen compounds using all the datasets for the binary ones included in our database. That is to say, if in a binary compound the element paired with hydrogen has the atomic number of Z , then the corresponding ternary compound is created by replacing it with the elements having $Z - 1$ and $Z + 1$ as follows: $H_6P(Z=15)Cl(Z=17)$ for $H_3S(Z=16)$, $Ba(Z=56)Ce(Z=58)H_{20}$ for $La(Z=57)H_{10}$, *etc.*. The values of S , h , P , and μ^* were matched to those of the corresponding binary data, in other word, only M were varied. Then, we calculated the x values of the hypothetical ternary compounds using the created datasets. Table I lists a part of the results on x and T_c for the hypothetical ternary compounds. We estimated the T_c values of the ternary compounds (T_c^t) using the relationship of $T_c^t = -0.8130(x^t - x^b) + T_c^b$, where x^t (x^b) is the evaluation value of the ternary (binary) compound and T_c^b is the T_c value of the binary compounds obtained by the Allen-Dynes formula⁷⁹, included in the database. The slope of -0.8130 is taken from a simple linear regression model, $y = -0.8130x + 1.66$, which is obtained by a least-

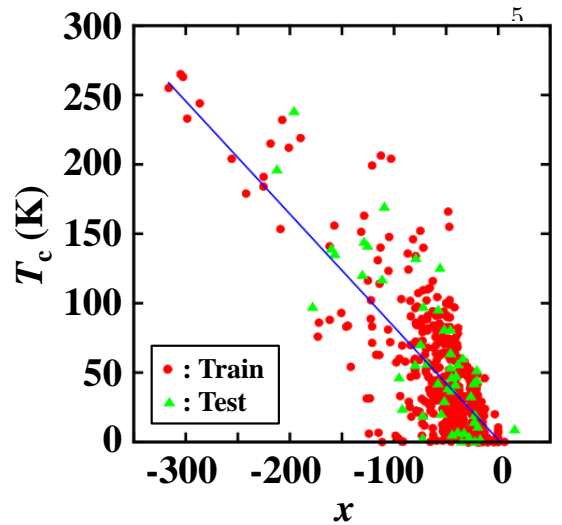


FIG. 9: (Color online) Correlation between T_c and the superconductivity evaluation value x calculated by the predictor. The training and testing data are represented as circle and triangle, respectively.

squares fitting of the data (see the line in Fig. 9). In the table, the results are classified into (a) the group 1-3 elements and (b) the group 13-16 elements. For the group 1-3 elements, in which polyhydrides with hydrogen cages are formed and T_c exceeds 200 K, the superconductivity is slightly suppressed for YH_{10} and MgH_6 and is less affected for LaH_{10} and AcH_{10} by changing to the hypothetical ternary compounds. Only CaH_{12} shows a slight enhancement of the superconductivity. For the group 13-16 elements, in which covalent hydrides are formed and T_c shows the values from 140 to 200 K, the superconductivity is largely suppressed for H_3S and SiH_3 , whereas it is less affected for AsH_8 , AlH_5 , and GeH_3 .

D. Validation of superconductivity from first principles: stages (i) and (ii) in MI cycle

1. $KScH_{12}$

We verified the superconductivity of one of the potential candidates, $KScH_{12}$, which is a hypothetical ternary compound approximated to CaH_6 and is included in the group 1-3 elements. CaH_6 is predicted to form the hydrogen cage structure under high pressure and show T_c of 220-235 K at 150 GPa, which is obtained by numerically solving the Eliashberg equations⁸⁰. Therefore, $KScH_{12}$ is expected to show similar crystal structure and superconductivity under high pressure.

The variation of T_c shown in Table I is estimated under the hypothesis that the space group S is invariant between binary and ternary compounds. However, S for the most stable structure of the ternary compound is

TABLE I: Superconductivity of the hypothetical ternary hydrogen compounds. The T_c values of the ternary compounds are estimated from the amount of change in the superconductivity evaluation value x .

compounds (S, h, P, μ^*)	x (M)	T_c (K)
(a) group 1-3		
YH ₁₀ → SrZrH ₂₀	-304.9 → -292.7	265 ⁶⁷ → 255
(229, 0.9091, 250, 0.10)	(9.00 → 9.05)	
MgH ₆ → NaAlH ₁₂	-302.6 → -287.5	263 ⁴⁸ → 251
(229, 0.8571, 300, 0.12)	(4.34 → 4.43)	
LaH ₁₀ → BaCeH ₂₀	-196.1 → -196.4	238 ⁶⁷ → 238
(225, 0.9091, 210, 0.10)	(13.54 → 13.53)	
CaH ₁₂ → KScH ₂₄	-112.6 → -113.7	206 ⁷⁴ → 207
(12, 0.9231, 150, 0.10)	(4.01 → 4.16)	
AcH ₁₀ → RaThH ₂₀	-102.9 → -102.6	204 ⁷⁵ → 204
(166, 0.9091, 200, 0.10)	(21.55 → 21.73)	
(b) group 13-16		
H ₃ S → H ₆ PdCl	-255.9 → -152.2	204 ³² → 120
(229, 0.7500, 200, 0.10)	(8.77 → 9.06)	
SiH ₃ → AlPH ₆	-209.1 → -50.2	153 ¹⁹ → 24
(221, 0.7500, 275, 0.10)	(7.78 → 8.00)	
AsH ₈ → GeSeH ₁₆	-131.6 → -131.6	151 ⁶³ → 151
(15, 0.8889, 450, 0.10)	(9.22 → 9.32)	
AlH ₅ → MgSiH ₁₀	-81.7 → -81.6	146 ⁴⁵ → 146
(11, 0.8333, 250, 0.10)	(5.34 → 5.21)	
GeH ₃ → GaAsH ₆	-71.9 → -72.1	140 ³¹ → 140
(223, 0.7500, 180, 0.13)	(18.91 → 18.84)	

considered to be different from that of the binary one. Therefore, first we searched for the most stable structure of KScH₁₂ by combining our GA code with the Quantum ESPRESSO (QE) code⁸¹ and applying it to KScH₁₂. In our GA search, 8 structures are created by “mating”, 6 “mutation (distortion)”, and 6 “mutation (permutation)” in each generation. We performed the structure search at pressures of 200 and 300 GPa, using calculation cells including 2 formula units. The generalized gradient approximation by Perdew, Burke and Ernzerhof⁸² was used for the exchange-correlation functional, and the Rabe-Rappe-Kaxiras-Joannopoulos ultrasoft pseudopotential⁸³ was employed. The k -space integration over the Brillouin zone (BZ) was carried out on a $4 \times 4 \times 4$ grid, and the energy cutoff was set at 80 Ry for the wave function and 640 Ry for the charge density. After we obtained the stable structures, we improved the calculation accuracy by increasing the number of k -points and checked the stability. As the results, we obtained a monoclinic $C2/m$ (No. 12) structure at 300 GPa, where it shows no phonon instability. The structure takes a modulated hydrogen-cage structure, similar to the structure of CaH₆ (compare the structure between the left and right in Fig. 10). The evaluation values of $Im-3m$ CaH₆ ($S = 229$)

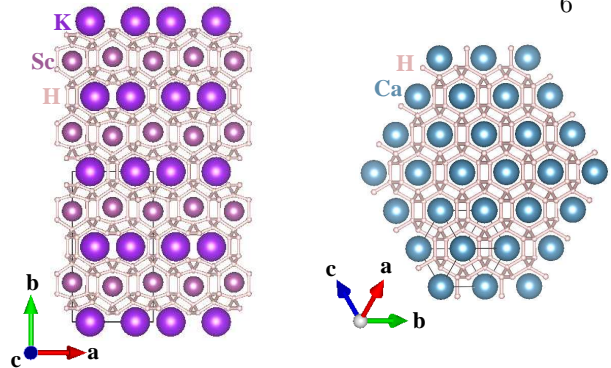


FIG. 10: (Color online) (Left) Crystal structure of KScH₁₂, predicted by GA. The space group is a monoclinic $C2/m$ (No. 12) with $a = 5.3726\text{\AA}$, $b/a = 1.7795$, $c/a = 0.5131$, $\beta = 106.6^\circ$, K: $4i$ (0.77998, 0, 0.47704), Sc: $4g$ (0, 0.26336, 0), H1: $8j$ (0.74515, 0.37079, 0.01997), H2: $8j$ (-0.05716, 0.43888, 0.14288), H3: $8j$ (0.57041, 0.41013, -0.05075), H4: $8j$ (0.81603, 0.18680, 0.40624), H5: $8j$ (0.68641, 0.18066, 0.59388), H6: $4h$ (0, 0.38665, 0.5), and H7: $4h$ (0, 0.84338, 0.5) at 300 GPa. (Right) Crystal structure of $Im-3m$ CaH₆ reported earlier⁸⁰. Crystal structures were drawn with VESTA⁸⁴.

TABLE II: Variation of superconductivity evaluation value x and superconducting T_c (ΔT_c) due to the change from $Im-3m$ CaH₆ to $C2/m$ KScH₁₂ at 300 GPa.

CaH ₆ → KScH ₁₂	x	ΔT_c (K)
$Im-3m \rightarrow C2/m$	-179.5 → -95.5	-68

and $C2/m$ KScH₁₂ ($S = 12$) are calculated to be -179.5 and -95.5 at 300 GPa, respectively (Table II). That is to say, T_c decreases by about 68 K owing to the change from $Im-3m$ CaH₆ to $C2/m$ KScH₁₂ according to the slope of -0.8130 mentioned in III C.

Next, we investigated the superconductivity of $C2/m$ KScH₁₂ using first-principles calculations. T_c was calculated using the Allen-Dynes formula⁷⁹,

$$T_c = \frac{\omega_{\log}}{1.2} \exp \left[-\frac{1.04(1 + \lambda)}{\lambda - \mu^*(1 + 0.62\lambda)} \right]. \quad (4)$$

In Eq. 4, the parameters of electron-phonon coupling constant λ and logarithmic-averaged phonon frequency ω_{\log} represent a set of characters for the phonon-mediated superconductivity. To obtain these parameters, we performed the phonon calculations implemented in the QE code. We used an $8 \times 16 \times 8$ k -point grid for the electron-phonon calculation, and $4 \times 8 \times 4$ k -point and $4 \times 4 \times 4$ q -point grids for the dynamical matrix calculation. We also calculated T_c of $Im-3m$ CaH₆ using a $24 \times 24 \times 24$ k -point, and $12 \times 12 \times 12$ k -point and $4 \times 4 \times 4$ q -point grids. The effective screened Coulomb repulsion constant μ^* was assumed to be 0.13, which has been considered to be a reasonable value for hydrides. The results are listed in Table III. T_c of $Im-3m$ CaH₆ at 150 GPa is

TABLE III: Superconductivity of CaH_6 and KScH_{12} , obtained by the first-principles calculations and the Allen-Dynes formula. T_c was calculated using $\mu^* = 0.13$.

	space group	P (GPa)	λ	ω_{ln}	T_c (K)
CaH_6	$Im-3m$ (No.229)	150	2.55	1091	172
		300	1.66	1388	160
KScH_{12}	$C2/m$ (No.12)	300	1.54	1139	122

TABLE IV: Variation of superconductivity evaluation value x and superconducting T_c (ΔT_c) due to the change from GeH_3 to GaAsH_6 at 180 GPa. The three datasets of GeH_3 , $Pm-3n$ (No. 223) GeH_3 , $Cccm$ (No. 66) GeH_3 , and $P4_2/mmc$ (No. 131), are taken from Ref.³¹.

$\text{GeH}_3 \rightarrow \text{GaAsH}_6$	x	ΔT_c (K)
$Cccm \rightarrow Pm-3$	-49.7 \rightarrow -40.0	-8
$P4_2/mmc \rightarrow Pm-3$	-48.8 \rightarrow -40.0	-7
$Pm-3n \rightarrow Pm-3$	-71.9 \rightarrow -40.0	-26

172 K, which is lower by about 50 K than that obtained by numerically solving the Eliashberg equations reported earlier⁸⁰. T_c of $C2/m$ KScH_{12} shows 122 K at 300 GPa, which is decreased by 38 K owing to the change from $Im-3m$ CaH_6 . This result indicates that the decrease of T_c is qualitatively consistent with that of estimated from the variation of the evaluation value x shown in Table II.

2. GaAsH_6

We verified the superconductivity of another candidate, GaAsH_6 , included in the group 13-16 elements. Gallium arsenide (GaAs) has been well known as a III-V direct semiconductor at ambient pressure, and the hydrogenation of the compound is expected to be achieved under high-pressure conditions, as well as group IV semiconductors. We searched for stable structures at pressures of 50, 100, 200, and 300 GPa, using calculation cells including 2 formula units. The k -space integration over the Brillouin zone (BZ) was performed on an $8 \times 8 \times 8$ grid, and the energy cutoff was set at 80 Ry for the wave function and 640 Ry for the charge density. As the results, we obtained a cubic $Pm-3$ (No. 200) structure at 180 GPa (Fig. 11). Although the structure is similar to the A15 structure with $Pm-3n$ (No. 223) of GeH_3 reported earlier³¹, the space group is different from that of the A15 structure. The evaluation value x of $Pm-3$ GaAsH_6 is calculated to be -40.0 at 180 GPa, which gives the T_c variations of -8 K from $Cccm$ GeH_3 , -7 K from $P4_2/mmc$ GeH_3 , and -26 K from $Pm-3n$ GeH_3 (Table IV). That is to say, T_c is slightly varied according to the change from $Cccm$ or $P4_2/mmc$ GeH_3 to $Pm-3$ GaAsH_6 , whereas it is more largely decreased according to the change from $Pm-3n$ GeH_3 .

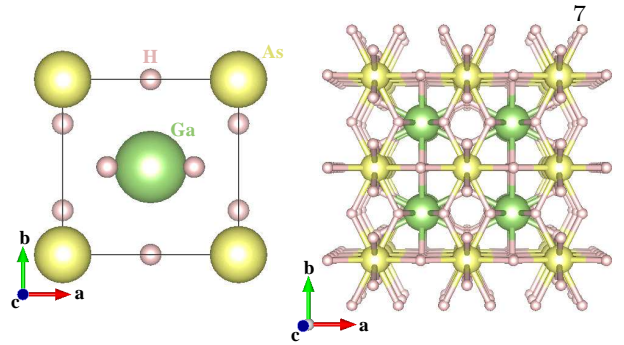


FIG. 11: (Color online) Crystal structure of GaAsH_6 , predicted by GA. The space group is a cubic $Pm-3$ (No. 200) with $a = 3.1050\text{\AA}$, Ga: $1b$ (0.5, 0.5, 0.5), As: $1a$ (0, 0, 0), and H: $6g$ (0.74736, 0.5, 0). Crystal structure was drawn with VESTA⁸⁴.

TABLE V: Superconductivity of GeH_3 and GaAsH_6 obtained by the first-principles calculations and the Allen-Dynes formula. The data of GeH_3 is taken from the Ref.³¹. T_c was calculated using $\mu^* = 0.13$.

	space group	P (GPa)	λ	ω_{ln}	T_c (K)
GeH_3	$Cccm$ (No.66)	180	1.60	793	100
	$P4_2/mmc$ (No.131)		1.56	737	90
	$Pm-3n$ (No.223)		1.82	989	140
GaAsH_6	$Pm-3$ (No.200)	180	1.57	897	98
		200	1.43	964	96
		300	1.57	635	69

We investigated the superconductivity of $Pm-3$ GaAsH_6 using first-principles calculations and the Allen-Dynes formula. We used a $48 \times 48 \times 48$ k -point grid for the electron-phonon calculation, and $24 \times 24 \times 24$ k -point and $6 \times 6 \times 6$ q -point grids for the dynamical matrix calculation. The effective screened Coulomb repulsion constant μ^* was assumed to be 0.13. The results are listed in Table V. T_c of $Pm-3$ GaAsH_6 shows 98 K at 180 GPa, which is lower by 42 K than that of a metastable $Pm-3n$ phase of GeH_3 ($T_c = 140$ K) but is comparable with that of the most stable $Cccm$ phase ($T_c = 100$ K). Thus, the T_c variations are qualitatively consistent with those estimated from the evaluation value x .

These results suggest that the regression analysis based on the superconductivity predictor gives reliable results on potential candidates for the high- T_c superconductivity in the ternary hydrogen compounds approximated to binary ones included in the database.

IV. DISCUSSION AND CONCLUSION

We developed the MI method consisting of the four stages, which is based on EA: (i) the stable structures are determined using GA, (ii) the physical and chemical

property data are collected by performing first-principles calculations for the stable structures, (iii) the functionality predictor is developed from the datasets in the database using GP, and (iv) potential candidates are discovered by the regression analysis. Turning of the cycle enables to accelerate the search for novel functional materials.

We applied the MI method to search for the superconductivity in hydrogen compounds. First, we developed the database on the superconductivity of the binary hydrogen compounds by collecting the data from literature. Then, we developed the superconductivity predictor and explored the superconductivity in the hypothetical ternary hydrogen compounds, approximated to the binary compounds included in the database. For the group 1-3 elements, the superconductivity is less affected by changing to the ternary compounds, and high- T_c superconductivity is expected in the hypothetical ternary compounds, as is the case with the binary ones. For the group 13-16 elements, the superconductivity is largely suppressed in the ternary compounds approximated to H_3S and SiH_3 , whereas those approximated to AsH_3 , AlH_3 , and GeH_3 are less affected by the changing. We actually verified the superconductivity of $KScH_{12}$ created from CaH_6 and $GaAsH_6$ created from GeH_3 using the first-principles calculations. For $KScH_{12}$, a modulated hydrogen-cage structure with a space group of $C2/m$ is obtained at 300 GPa by GA, and T_c shows 122 K for $\mu^* = 0.13$. For $GaAsH_6$, we predicted a cubic $Pm-3$

structure and obtained T_c of 98 K at 180 GPa. These T_c values are qualitatively consistent with those estimated from the variations of the superconductivity evaluation values. These results suggest that the regression analysis based on the superconductivity predictor is effective for the discovery of potential candidates in the ternary hydrogen compounds.

The prediction ability of the superconductivity in ternary hydrogen compounds is expected to be further improved by aggregating the superconductivity data of $KScH_{12}$, $GaAsH_6$, and other ternary compounds into the database and redeveloping the predictor by GP. At present, the superconductivity of $T_c \geq 200$ K is found only in the pressure above 150 GPa. Therefore, the achievement of more than 200 K superconductivity at low pressure is also significantly important, and MI approaches could be effective for the research.

Acknowledgments

This work was supported by JSPS KAKENHI under Grant-in-Aid for Specially Promoted Research (26000006), Scientific Research (C) (17K05541), and Scientific Research (S) (16H06345), Asahi Glass Foundation, Yamada Science Foundation, and MEXT as “Exploratory Challenge on Post-K computerh (Frontiers of Basic Science: Challenging the Limits).

-
- * Electronic address: ISHIKAWA.Takahiro@nims.go.jp
- ¹ R. Potyrailo, K. Rajan, K. Stoewe, I. Takeuchi, and B. Chisholm, *ACS Comb. Sci.* **13**, 579 (2011).
 - ² A. Jain, S. P. Ong, G. Hautier, W. Chen, W. D. Richards, S. Dacek, S. Cholia, D. Gunter, D. Skinner, G. Ceder, et al., *APL Materials* **1**, 011002 (2013).
 - ³ S. P. Ong, W. D. Richards, A. Jain, G. Hautier, M. Kocher, S. Cholia, D. Gunter, V. L. Chevrier, K. A. Persson, and G. Ceder, *Comput. Mater. Sci.* **68**, 314 (2013).
 - ⁴ K. Takahashi and Y. Tanaka, *Dalton Trans.* **2**, 10497 (2016).
 - ⁵ M. Nishijima, T. Ootani, Y. Kamimura, T. Sueki, S. Esaki, S. Murai, K. Fujita, K. Tanaka, K. Ohira, Y. Koyama, et al., *Nat. Commun.* **5**, 4553 (2014).
 - ⁶ V. Stanev, C. Oses, A. G. Kusne, E. Rodriguez, J. Paglione, S. Curtarolo, and I. Takeuchi, *Npj Comput. Mater.* **4**, 29 (2018).
 - ⁷ D. M. Deaven and K. M. Ho, *Phys. Rev. Lett.* **75**, 288 (1995).
 - ⁸ T. S. Bush, C. R. A. Catlow, and P. D. Battle, *J. Mater. Chem.* **5**, 1269 (1995).
 - ⁹ S. M. Woodley, P. D. Battle, J. D. Gale, and C. R. A. Catlow, *Phys. Chem. Chem. Phys.* **1**, 2535 (1999).
 - ¹⁰ S. M. Woodley, *Struct. Bonding* **110**, 95 (2004).
 - ¹¹ A. R. Oganov and C. W. Glass, *J. Chem. Phys.* **124**, 244704 (2006).
 - ¹² M. Stone, *J. Royal Stat. Soc.* **36**, 111 (1974).
 - ¹³ A. P. Drozdov, M. I. Erements, I. A. Troyan, V. Kseno-
fontov, and S. I. Shylin, *Nature* **525**, 73 (2015).
 - ¹⁴ A. P. Drozdov, P. P. Kong, V. S. Minkov, S. P. Besedin, M. A. Kuzovnikov, S. Mozaffari, L. Balicas, F. F. Balakirev, D. E. Graf, V. B. Prakapenka, et al., *Nature* **569**, 528 (2019).
 - ¹⁵ M. Somayazulu, M. Ahart, A. K. Mishra, Z. M. Geballe, M. Baldini, Y. Meng, V. V. Struzhkin, and R. J. Hemley, *Phys. Rev. Lett.* **122**, 027001 (2019).
 - ¹⁶ X.-J. Chen, J.-L. Wang, V. V. Struzhkin, H. k. Mao, R. J. Hemley, and H.-Q. Lin, *Phys. Rev. Lett.* **101**, 077002 (2008).
 - ¹⁷ D. Y. Kim, R. H. Scheicher, and R. Ahuja, *Phys. Rev. Lett.* **103**, 077002 (2009).
 - ¹⁸ J. S. Tse, Z. Song, Y. Yao, J. S. Smith, S. Desgreniers, and D. D. Klug, *Solid State Commun.* **149**, 1944 (2009).
 - ¹⁹ X. Jin, X. Meng, Z. He, Y. Ma, B. Liu, T. Cui, G. Zou, and H. k. Mao, *Proc. Natl. Acad. Sci. USA* **107**, 9969 (2010).
 - ²⁰ D. Duan, F. Tian, Z. He, X. Meng, L. Wang, C. Chen, X. Zhao, B. Liu, and T. Cui, *J. Chem. Phys.* **133**, 074509 (2010).
 - ²¹ G. Gao, A. R. Oganov, P. Li, Z. Li, H. Wang, T. Cui, Y. Ma, A. Bergara, A. O. Lyakhov, T. Iitaka, et al., *Proc. Natl. Acad. Sci. USA* **107**, 1317 (2010).
 - ²² D. Y. Kim, R. H. Scheicher, C. J. Pickard, R. J. Needs, and R. Ahuja, *Phys. Rev. Lett.* **107**, 117002 (2011).
 - ²³ G. Gao, H. Wang, A. Bergara, Y. Li, G. Liu, and Y. Ma, *Phys. Rev. B* **84**, 064118 (2011).
 - ²⁴ K. Abe and N. W. Ashcroft, *Phys. Rev. B* **84**, 104118

- (2011).
- 25 C. Zhang, X.-J. Chen, and H.-Q. Lin, *J. Phys.: Condens. Matter* **24**, 035701 (2012).
 - 26 D. Zhou, X. Jin, X. Meng, G. Bao, Y. Li, B. Liu, and T. Cui, *Phys. Rev. B* **86**, 014118 (2012).
 - 27 D. C. Lonie, J. Hooper, B. Altintas, and E. Zurek, *Phys. Rev. B* **87**, 054107 (2013).
 - 28 G. Gao, R. Hoffmann, N. W. Ashcroft, H. Liu, A. Bergara, and Y. Ma, *Phys. Rev. B* **88**, 184104 (2013).
 - 29 C.-H. Hu, A. R. Oganov, Q. Zhu, G.-R. Qian, G. Frapper, A. O. Lyakhov, and H.-Y. Zhou, *Phys. Rev. Lett.* **110**, 165504 (2013).
 - 30 J. Hooper, B. Altintas, A. Shamp, and E. Zurek, *J. Phys. Chem. C* **117**, 2982 (2013).
 - 31 K. Abe and N. W. Ashcroft, *Phys. Rev. B* **88**, 174110 (2013).
 - 32 D. Duan, Y. Liu, F. Tian, D. Li, X. Huang, Z. Zhao, H. Yu, B. Liu, W. Tian, and T. Cui, *Sci. Rep.* **4**, 6968 (2014).
 - 33 C. Chen, F. Tian, D. Duan, K. Bao, X. Jin, B. Liu, and T. Cui, *J. Chem. Phys.* **140**, 114703 (2014).
 - 34 I. Errea, M. Calandra, and F. Mauri, *Phys. Rev. B* **89**, 064302 (2014).
 - 35 S. Yu, Q. Zeng, A. R. Oganov, C. Hu, G. Frapper, and L. Zhang, *AIP Advances* **4**, 107118 (2014).
 - 36 Y. Li, J. Hao, H. Liu, Y. Li, and Y. Ma, *J. Chem. Phys.* **140**, 174712 (2014).
 - 37 Y. Xie, Q. Li, A. R. Oganov, and H. Wang, *Acta Cryst. C* **70**, 104 (2014).
 - 38 Z. Wang, Y. Yao, L. Zhu, H. Liu, T. Iitaka, H. Wang, and Y. Ma, *J. Chem. Phys.* **140**, 124707 (2014).
 - 39 C. Chen, Y. Xu, X. Sun, and S. Wang, *J. Phys. Chem. C* **119**, 17039 (2015).
 - 40 D. Duan, F. Tian, Y. Liu, X. Huang, D. Li, H. Yu, Y. Ma, B. Liu, and T. Cui, *Phys. Chem. Chem. Phys.* **17**, 32335 (2015).
 - 41 A. Shamp and E. Zurek, *J. Phys. Chem. Lett.* **6**, 4067 (2015).
 - 42 H. Zhang, X. Jin, Y. Lv, Q. Zhuang, Q. Lv, Y. Liu, K. Bao, D. Li, B. Liu, and T. Cui, *Phys. Chem. Chem. Phys.* **17**, 27630 (2015).
 - 43 H. Zhang, X. Jin, Y. Lv, Q. Zhuang, Y. Liu, Q. Lv, K. Bao, D. Li, B. Liu, and T. Cui, *Sci. Rep.* **5**, 8845 (2015).
 - 44 I. Errea, M. Calandra, C. J. Pickard, J. Nelson, R. J. Needs, Y. Li, H. Liu, Y. Zhang, Y. Ma, and F. Mauri, *Phys. Rev. Lett.* **114**, 157004 (2015).
 - 45 P. Hou, X. Zhao, F. Tian, D. Li, D. Duan, Z. Zhao, B. Chu, B. Liu, and T. Cui, *RSC Adv.* **5**, 5096 (2015).
 - 46 S. Yu, X. Jia, G. Frapper, D. Li, A. R. Oganov, Q. Zeng, and L. Zhang, *Sci. Rep.* **5**, 17764 (2015).
 - 47 S. Zhang, Y. Wang, J. Zhang, H. Liu, X. Zhong, H.-F. Song, G. Yang, L. Zhang, and Y. Ma, *Sci. Rep.* **5**, 15433 (2015).
 - 48 X. Feng, J. Zhang, G. Gao, H. Liu, and H. Wang, *RSC Adv.* **5**, 59292 (2015).
 - 49 X. Yan, Y. Chen, X. Kuang, and S. Xiang, *J. Chem. Phys.* **143**, 124310 (2015).
 - 50 Y. Cheng, C. Zhang, T. Wang, G. Zhong, C. Yang, X.-J. Chen, and H.-Q. Lin, *Sci. Rep.* **5**, 16475 (2015).
 - 51 Y. Liu, D. Duan, F. Tian, D. Li, X. Sha, Z. Zhao, H. Zhang, G. Wu, H. Yu, B. Liu, et al., *arXiv:1503.08587* (2015).
 - 52 Y. Liu, D. Duan, F. Tian, H. Liu, C. Wang, X. Huang, D. Li, Y. Ma, B. Liu, and T. Cui, *Inorg. Chem.* **54**, 9924 (2015).
 - 53 Y. Liu, D. Duan, X. Huang, F. Tian, D. Li, X. Sha, C. Wang, H. Zhang, T. Yang, B. Liu, et al., *J. Phys. Chem. C* **119**, 15905 (2015).
 - 54 Y. Liu, X. Huang, D. Duan, F. s, H. Liu, D. Li, Z. Zhao, X. Sha, H. Yu, H. Zhang, et al., *Sci. Rep.* **5**, 11381 (2015).
 - 55 Y. Ma, D. Duan, D. Li, Y. Liu, F. Tian, H. Yu, C. Xu, Z. Shao, B. Liu, and T. Cui, *arXiv:1511.05291* (2015).
 - 56 A. Shamp, T. Terpstra, T. Bi, Z. Falls, P. Avery, and E. Zurek, *J. Am. Chem. Soc.* **138**, 1884 (2016).
 - 57 H. Liu, Y. Li, G. Gao, J. S. Tse, and I. I. Naumov, *J. Phys. Chem. C* **120**, 3458 (2016).
 - 58 G.-R. Qian, H. Niu, C.-H. Hu, A. R. Oganov, Q. Zeng, and H.-Y. Zhou, *arXiv:1411.4513* (2016).
 - 59 M. M. D. Esfahani, Z. Wang, A. R. Oganov, H. Dong, Q. Zhu, S. Wang, M. S. Rikitin, and X.-F. Zhou, *Sci. Rep.* **6**, 22873 (2016).
 - 60 T. Ishikawa, A. Nakanishi, K. Shimizu, H. Katayama-Yoshida, T. Oda, and N. Suzuki, *Sci. Rep.* **6**, 23160 (2016).
 - 61 X. Li, H. Liu, and F. Peng, *Phys. Chem. Chem. Phys.* **18**, 28791 (2016).
 - 62 X. Zhong, H. Wang, J. Zhang, H. Liu, S. Zhang, H.-F. Song, G. Yang, L. Zhang, and Y. Ma, *Phys. Rev. Lett.* **116**, 057002 (2016).
 - 63 Y. Fu, X. Du, L. Zhang, F. Peng, M. Zhang, C. J. Pickard, R. J. Needs, D. J. Singh, W. Zheng, and Y. Ma, *Chem. Mater.* **28**, 1746 (2016).
 - 64 Y. Li, L. Wang, H. Liu, Y. Zhang, J. Hao, C. J. Pickard, J. R. Nelson, R. J. Needs, W. Li, Y. Huang, et al., *Phys. Rev. B* **93**, 020103(R) (2016).
 - 65 Y. Liu, D. Duan, F. Tian, C. Wang, Y. Ma, D. Li, X. Huang, B. Liu, and T. Cui, *Phys. Chem. Chem. Phys.* **18**, 1516 (2016).
 - 66 A. Majumdar, J. S. Tse, M. Wu, and Y. Yao, *Phys. Rev. B* **96**, 201107(R) (2017).
 - 67 H. Liu, I. I. Naumov, R. Hoffmann, N. W. Ashcroft, and R. J. Hemley, *Proc. Natl. Acad. Sci. USA* **114**, 6990 (2017).
 - 68 M. M. D. Esfahani, A. R. Oganov, H. Niu, and J. Zhang, *arXiv:1701.05600* (2017).
 - 69 Q. Zeng, S. Yu, D. Li, A. R. Oganov, and G. Frappere, *Phys. Chem. Chem. Phys.* **19**, 8236 (2017).
 - 70 Q. Zhuang, X. Jin, T. Cui, Y. Ma, Q. Lv, Y. Li, H. Zhang, X. Meng, and K. Bao, *Inorg. Chem.* **56**, 3901 (2017).
 - 71 T. Ishikawa, A. Nakanishi, K. Shimizu, and T. Oda, *J. Phys. Soc. Jpn.* **86**, 124711 (2017).
 - 72 X. Li and F. Peng, *Inorg. Chem.* **56**, 13759 (2017).
 - 73 X.-F. Li, Z.-Y. Hu, and B. Huang, *Phys. Chem. Chem. Phys.* **19**, 3538 (2017).
 - 74 D. V. Semenov, I. A. Kruglov, A. G. Kvashnin, and A. R. Oganov, *arXiv:1806.00865* (2018).
 - 75 D. V. Semenov, A. G. Kvashnin, I. A. Kruglov, and A. R. Oganov, *J. Phys. Chem. Lett.* **9**, 1920 (2018).
 - 76 K. V. Shanavas, L. Lindsay, and D. S. Parker, *Sci. Rep.* **6**, 28102 (2018).
 - 77 L. Wang, D. Duan, H. Yu, H. Xie, X. Huang, Y. Ma, F. Tian, D. Li, B. Liu, and T. Cui, *Inorg. Chem.* **57**, 181 (2018).
 - 78 X. Ye, N. Zarifi, E. Zurek, R. Hoffmann, and N. W. Ashcroft, *J. Phys. Chem. C* **122**, 6298 (2018).
 - 79 P. B. Allen and R. C. Dynes, *Phys. Rev. B* **12**, 905 (1975).
 - 80 H. Wang, J. S. Tse, K. Tanaka, T. Iitaka, and Y. Ma, *Proc. Natl. Acad. Sci. USA* **109**, 6463 (2012).
 - 81 P. Giannozzi, S. Baroni, N. Bonini, M. Calandra, R. Car, C. Cavazzoni, D. Cereso, G. L. Chiarott, M. Cococcioni, I. Dabo, et al., *J. Phys.: Condens. Matter* **21**, 395502 (2009).

- ⁸² J. P. Perdew, K. Burke, and M. Ernzerhof, Phys. Rev. Lett. **77**, 3865 (1996).
- ⁸³ A. M. Rappe, K. M. Rabe, E. Kaxiras, and J. D. Joannopoulos, Phys. Rev. B **41**, 1227 (1990).
- ⁸⁴ K. Momma and F. Izumi, J. Appl. Crystallogr. **44**, 1272 (2011).